Polynuclear Nickel(II) Complexes: Preparation and Magnetic Properties of Ni^{II}_4, Ni^{II}_5, and Ni^{II}_6 Species with Ligands containing O∩X∩O (X = S, Se or N) Donor Atoms

Tapan K. Paine,[a] Eva Rentschler,[a] Thomas Weyhermüller,[a] and Phalguni Chaudhuri*[a]

Keywords: Magnetic properties / Nickel / Selenium / Sulfur / Tripodal ligands

A family of bisphenol-containing ligands with XO_2 donor atoms, where X = S, Se, or N, yields $[Ni^{II}]_4$ (**1**) and (**2**), $[Ni^{II}]_5$ (**3**), and $[Ni^{II}]_6$ (**4**) complexes. Complex **2**, **3**, and **4** have been structurally characterised by X-ray diffraction. The compounds were characterised spectroscopically and by variable-temperature (2–295 K), variable-field (1, 4, and 7 T) magnetic susceptibility measurements. Analysis of the magnetic data shows predominant ferromagnetic interactions between the nickel centres (S_{Ni} = 1) indicating "high-spin" ground states for **1**, **2**, and **3**, whereas complex **4** shows antiferromagnetic interactions. A plot of J vs. Ni–O–Ni angles for all structurally characterised Ni_4O_4 cubane cores, including **2**, irrespective of their symmetry, shows a large variation of J values within a small range of Ni–O–Ni angles. A simple two-J model was found to be adequate to describe the magnetic properties of the hexanuclear complex, **4**.

Introduction

There are several intriguing features associated with polynuclear transition metal complexes. Firstly, these complexes can have unusual electronic properties and may serve as sources of fundamental information about exchange coupling in multinuclear assemblies. A second general reason to study polynuclear metal complexes is that they may be building blocks for molecularly based magnetic materials. In another field of coordination chemistry, polynuclear complexes are important for the advancement of bioinorganic chemistry, both in their roles in advancing understanding of the chemistry of metallobiomolecules[1] and in the production of useful new biomimetic and bioinspired reactions. The magnetic molecular assemblies are therefore of interest for research areas as different as biochemistry and molecular magnetism.[2] These potential applications and issues have sparked and fuelled the interest of coordination chemists in synthesising molecules with large numbers of unpaired electrons in ground states. Consequently, the search for ligands capable of giving rise to molecules of high nuclearity is an important theme in modern coordination chemistry.

We have been exploring the feasibility of using phenol-containing ligands[3−6] to influence the nuclearity and topology of metal complexes. Since nickel(II) is known to have a large single-ion zero-field splitting and often gives rise to ferromagnetic coupling, we have especially focussed our attention on polynuclear nickel(II) complexes[7] with the aim of obtaining "high spin" species. Although polynuclear nickel(II) complexes containing up to four metal ions are not rare,[8−9] assemblies with five,[10] six,[11] and more[12] nickel(II) ions still remain a matter of curiosity. In this paper we report on the extension of our studies with the ligands containing the donor atoms (O, X, O), where X = S, Se, or N, and include the preparation and magnetochemical characterisation of

$[Ni^{II}_4L^S_2(\mu_3\text{-OMe})_4(MeOH)_4(MeCN)_2]$ (**1**),
$[Ni^{II}_4L^{Se}_2(\mu_3\text{-OMe})_4(MeOH)_4(MeCN)_2]$ (**2**),
$[Ni^{II}_5L^N_4(\mu_3\text{-OH})_2(\mu_2\text{-OH}_2)_2(EtOH)_2]$ (**3**),

and

$[Ni^{II}_6L^N_4(\mu_2\text{-OHMe})(\mu_3\text{-OMe})_2(\mu_3\text{-OH})_2(MeOH)_2(MeCN)_2]$ (**4**),

where H_2L^S is 2,2′-thiobis(4,6-di-*tert*-butylphenol), H_2L^{Se} is 2,2′-selenobis(4,6-di-*tert*-butylphenol), and H_2L^N is methylamino-*N*,*N*-bis(2-methylene-4,6-dimethylphenol).

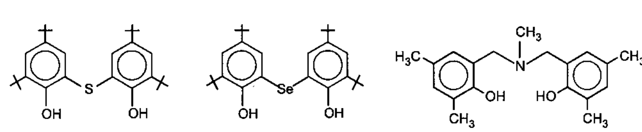

H_2L^S H_2L^{Se} H_2L^N

Results and Discussion

Depending on the solvents and the bases used during the preparations, complexes **1−4** were isolated in good yields (Scheme 1). The sulfur- and selenium-containing ligands, H_2L^S and H_2L^{Se}, reacted with $NiCl_2{\cdot}6H_2O$ at room tem-

[a] Max-Planck-Institut für Bioanorganische Chemie, Stiftstrasse 34−36, 45470 Mülheim an der Ruhr, Germany
E-mail: Chaudh@mpi-muelheim.mpg.de

 DOI: 10.1002/ejic.200300164

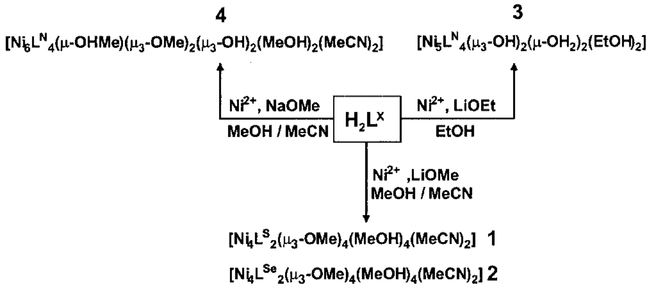

Scheme 1

perature in a solvent mixture (5:1) of methanol and acetonitrile containing $LiOCH_3$ as the base to deprotonate the phenolic −OH groups, from which complexes **1** and **2**, respectively, were isolated. On the other hand, treatment of the nitrogen-containing ligand H_2L^N with $NiCl_2{\cdot}6H_2O$ in ethanol in the presence of the base $LiOC_2H_5$ resulted in a yellow-green microcrystalline solid, which on subsequent recrystallisation from a solvent mixture (1:2) of CH_2Cl_2 and C_2H_5OH yielded pure pentanuclear material **3** in a good isolated yield of 75%. The incorporation of OH^- and H_2O in **3** presumably implies the involvement of water from the starting material. Interestingly, the isolation of the green **4**, a Ni^{II}_6 species, from a solvent mixture of methanol and acetonitrile was particularly sensitive to the use of dry solvents, although the starting material was a hydrated metal salt. This indicates that complex **4** appears in the reaction mixture only at water concentrations considerably lower than present in the case of complex **3**, and hence the absence of water as ligands in the final product **4**. That the isolated complexes **1**−**4** are thermodynamic products is shown by the reactions' insensitivity to the ligand/Ni^{II} ratios, which vary between 2:1 to 0.5:1.

Selected IR data for complexes **1**−**4** are given in the Exp. Sect. The sharp ν(OH) band around 3400 cm^{-1} for the free ligands is replaced by a broad band, indicating that the phenol character of the ligand has been lost on complexation. There are several strong bands in the 2960−2820 cm^{-1} region, due to the ν(C−H) stretchings of the *tert*-butyl groups. The weak bands in the 2300−2250 cm^{-1} region correspond to the ν(CN) vibrations of the CH_3CN molecule. The strong sharp band at 1047 cm^{-1} for both **1** and **2** is attributed to the $\nu(OCH_3)$ group of the bridging methoxide ligand.[19] The corresponding band at 1057 cm^{-1} for **4** appears as a medium band. The other ν(C−H), ν(C=C), and ν(C−O) vibrations are found in the normal ranges for these types of linkages.

Mass spectrometry in the EI and ESI mode has not proved to be a useful analytical tool for characterisation of the polynuclear Ni^{II} complexes **1**−**4**, presumably due to their decomposition at the temperatures applied in mass spectrometry.

Single-Crystal X-ray Diffraction Studies

The analytical, spectroscopic and magnetic data for **1** and **2** showed their isostructural characters, so X-ray analysis only of **2** was undertaken, to remove the doubts regarding connectivity.

Molecular Structure of 2

The crystal structure of **2** is shown in Figure 1, with selected bond lengths and angles provided in Table 1. The solid-state structure of **2**·3.5MeCN·0.5MeOH contains discrete

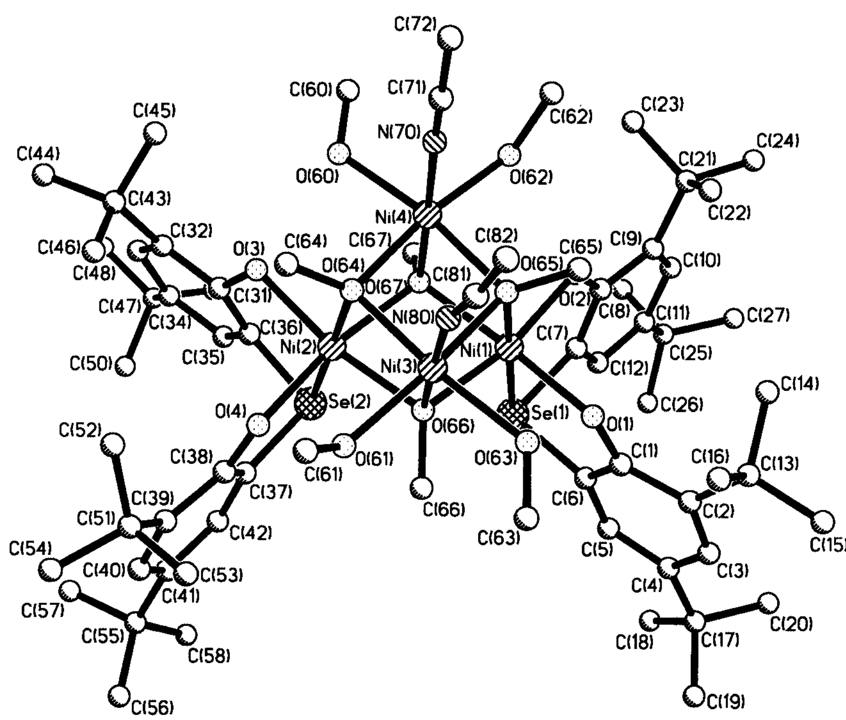

Figure 1. Molecular structure of $[Ni_4L^{Se}_2(\mu_3\text{-}OMe)_4(MeOH)_4(MeCN)_2]$ (**2**)

Table 1. Selected bond lengths [Å] and angles [deg] for $[Ni_4L^{Se}{}_2(\mu_3\text{-}OMe)_4(MeOH)_4(MeCN)_2]\cdot 3.5MeCN\cdot 0.5MeOH$ (**2**)

Ni(1)−O(1)	2.039(2)	O(1)−Ni(1)−O(2)	96.49(10)
Ni(1)−O(2)	2.047(2)	O(1)−Ni(1)−O(65)	90.69(9)
Ni(1)−O(65)	2.056(2)	O(2)−Ni(1)−O(65)	95.73(9)
Ni(1)−O(67)	2.073(2)	O(1)−Ni(1)−O(67)	170.61(9)
Ni(1)−O(66)	2.093(2)	O(2)−Ni(1)−O(67)	90.35(9)
Ni(1)−Se(1)	2.4452(6)	O(65)−Ni(1)−O(67)	82.20 (9)
Ni(2)−O(3)	2.054(2)	O(1)−Ni(1)−O(66)	94.52(9)
Ni(2)−O(64)	2.058(2)	O(2)−Ni(1)−O(66)	168.72(9)
Ni(2)−O(4)	2.060(2)	O(65)−Ni(1)−O(66)	81.69(9)
Ni(2)−O(66)	2.074(2)	O(67)−Ni(1)−O(66)	78.44(9)
Ni(2)−O(67)	2.082(2)	O(1)−Ni(1)−Se(1)	86.57(7)
Ni(2)−Se(2)	2.4480(6)	O(2)−Ni(1)−Se(1)	86.90(7)
Ni(3)−O(66)	2.011(2)	O(65)−Ni(1)−Se(1)	176.40(7)
Ni(3)−O(65)	2.036(2)	O(67)−Ni(1)−Se(1)	100.26(6)
Ni(3)−O(64)	2.043(2)	O(66)−Ni(1)−Se(1)	96.19(6)
Ni(3)−O(63)	2.058(3)	O(3)−Ni(2)−O(64)	92.07(9)
Ni(3)−O(61)	2.073(3)	O(3)−Ni(2)−O(4)	97.97(10)
Ni(3)−N(80)	2.074(3)	O(64)−Ni(2)−O(4)	95.42(9)
Ni(4)−O(67)	2.031(2)	O(3)−Ni(2)−O(66)	169.84(10)
Ni(4)−O(65)	2.034(2)	O(64)−Ni(2)−O(66)	82.10(9)
Ni(4)−O(64)	2.043(2)	O(4)−Ni(2)−O(66)	90.88(10)
Ni(4)−O(60)	2.054(3)	O(3)−Ni(2)−O(67)	92.34(10)
Ni(4)−N(70)	2.066(3)	O(64)−Ni(2)−O(67)	82.12(9)
Ni(4)−O(62)	2.076(3)	O(4)−Ni(2)−O(67)	169.48(10)
		O(66)−Ni(2)−O(67)	78.66(9)
		O(3)−Ni(2)−Se(2)	86.51(7)
Ni(3)−O(64)−Ni(4)	96.93(10)	O(64)−Ni(2)−Se(2)	177.83(7)
Ni(3)−O(64)−Ni(2)	95.94(10)	O(4)−Ni(2)−Se(2)	86.40(7)
Ni(4)−O(64)−Ni(2)	96.54(10)	O(66)−Ni(2)−Se(2)	99.07(6)
Ni(4)−O(65)−Ni(3)	97.44(10)	O(67)−Ni(2)−Se(2)	96.30(6)
Ni(4)−O(65)−Ni(1)	96.40(9)	O(66)−Ni(3)−O(65)	84.22(9)
Ni(3)−O(65)−Ni(1)	96.48(10)	O(66)−Ni(3)−O(64)	84.06(9)
Ni(3)−O(66)−Ni(2)	96.41(10)	O(65)−Ni(3)−O(64)	82.71(10)
Ni(3)−O(66)−Ni(1)	96.09(9)	O(66)−Ni(3)−O(63)	89.18(10)
Ni(2)−O(66)−Ni(1)	101.05(10)	O(65)−Ni(3)−O(63)	88.37(10)
Ni(4)−O(67)−Ni(1)	95.93(9)	O(64)−Ni(3)−O(63)	169.29(10)
Ni(4)−O(67)−Ni(2)	96.15(10)	O(66)−Ni(3)−O(61)	88.15(10)
Ni(1)−O(67)−Ni(2)	101.45(10)	O(65)−Ni(3)−O(61)	170.29(10)
		O(64)−Ni(3)−O(61)	90.55(10)
Ni(1)···Ni(2)	3.217(2)	O(63)−Ni(3)−O(61)	97.54(11)
Ni(1)···Ni(3)	3.052(2)	O(66)−Ni(3)−N(80)	177.73(11)
Ni(1)···Ni(4)	3.049(2)	O(65)−Ni(3)−N(80)	93.72(12)
Ni(2)···Ni(3)	3.046(2)	O(64)−Ni(3)−N(80)	96.63(12)
Ni(2)···Ni(4)	3.061(2)	O(63)−Ni(3)−N(80)	89.82(12)
Ni(3)···Ni(4)	3.058(2)	O(61)−Ni(3)−N(80)	93.99(12)
		O(67)−Ni(4)−O(65)	83.80(9)
		O(67)−Ni(4)−O(64)	83.75(9)
		O(65)−Ni(4)−O(64)	82.75(10)
		O(67)−Ni(4)−O(60)	89.06(10)
		O(65)−Ni(4)−O(60)	170.10(10)
		O(64)−Ni(4)−O(60)	89.69(10)
		O(67)−Ni(4)−N(70)	178.40(11)
		O(65)−Ni(4)−N(70)	96.09(11)
		O(64)−Ni(4)−N(70)	94.65(11)
		O(60)−Ni(4)−N(70)	90.86(12)
		O(67)−Ni(4)−O(62)	88.87(10)
		O(65)−Ni(4)−O(62)	90.73(10)
		O(64)−Ni(4)−O(62)	170.63(10)
		O(60)−Ni(4)−O(62)	95.99(11)
		N(70)−Ni(4)−O(62)	92.73(12)

tetrameric molecules of formula $[Ni_4L^{Se}{}_2(\mu_3\text{-}OMe)_4(MeOH)_4(MeCN)_2]$, based on a Ni_4O_4 cubane-type unit and consisting of two interpenetrating tetrahedra: one of four nickel atoms and one of four μ_3-oxygen atoms originating from bridging methoxide groups. Each Ni^{II} is in a distorted octahedral environment and bound to three μ_3-OCH_3 ligands. For Ni(1) and Ni(2), two facially coordinated O∩Se∩O donor sets of the deprotonated ligands $[L^{Se}]^{2-}$ complete the sixfold coordination. Each Ni(3) and Ni(4) is coordinated to three bridging methoxide oxygens and two terminal MeOH ligands. The sixth coordination site in each nickel centre is occupied by a N-atom of a terminal MeCN molecule. Although it was not possible to locate all the hydrogen atoms in the structure, the intramolecular contacts between the oxygen atoms of the methanol molecules and the oxygen atoms of the phenolate groups of the ancillary $[L^{Se}]^{2-}$ ligand − of ca. 2.70 Å [O(1)···O(63) 2.674 Å; O(2)···O(62) 2.718 Å; O(3)···O(60) 2.702 Å; O(4)···O(61) 2.720 Å] − can be interpreted as hydrogen bonds. The intramolecular hydrogen bonds have the effect of lowering the effective symmetry of the $[Ni_4(OMe)_4]$-core from T_d *to* D_{2d}.

A similar pattern of intramolecular hydrogen bonding and structural distortions have also been observed in other alkoxide cubane complexes containing Ni^{II} and bound alcohol. The Ni−O−Ni angles in **2** vary between 95.9(1) and 101.5(1)°. The Ni···Ni distances on different cubic faces are also different, the shortest being Ni(3)···Ni(2) 3.046(2) Å and the longest Ni(1)···Ni(2) 3.217(2) Å. Average Ni−O bond lengths of 2.045 Å (phenolate) and 2.075 Å (methoxide) lie well within the range of reported[4,8] values for the corresponding bond lengths of the tetranuclear cubane-like Ni^{II}. All phenyl rings of the ligands are planar and retain their aromaticity after complexation. No substantial differences in bond lengths and angles are found between the two crystallographically independent molecules.

Molecular Structure of 3

The molecular structure of **3** is shown in Figure 2. Selected interatomic distances and bond angles are listed in Table 2. The solid-state structure of $\mathbf{3}\cdot 0.75CH_2Cl_2$ contains discrete pentanuclear molecules of formula $[Ni_5L^N{}_4(\mu_3\text{-}OH)_2(\mu_2\text{-}OH_2)_2(EtOH)_2]$. The structure can be regarded as a corner-shared dicubane, in which one of the corners of each cubane is missing. The pentanuclear assembly is composed of a Ni_2−Ni−Ni_2 array; there is a virtually twofold axis passing through the central Ni(3). There are two different types of peripheral Ni atoms: the five-coordinate Ni(2) and Ni(5) with a NO_4 square-pyramidal environment and the six-coordinate Ni(1) and Ni(4) in a distorted octahedral NO_5 environment. The peripheral metal atoms, Ni(1), Ni(2), Ni(4), and Ni(5), are bound equatorially to the deprotonated ancillary ligand $[L^N]^{2-}$. Two μ_3-hydroxide ions [O(100) for Ni(2) and O(200) for Ni(5)] act as the axial donor atoms of the square pyramids. That the donor atoms O(101) and O(201) are constituents of water molecules is discernible from the Ni−O bond lengths. Furthermore, the hydrogen atoms of the water molecules and of hydroxy groups were located from a difference map and are shown as circles of arbitrary radii in Figure 2. Two ethanol molecules, O(300) and O(400), are bound as terminal ions to Ni(1) and Ni(4), respectively, *trans* to the μ_2-OH_2 ligands.

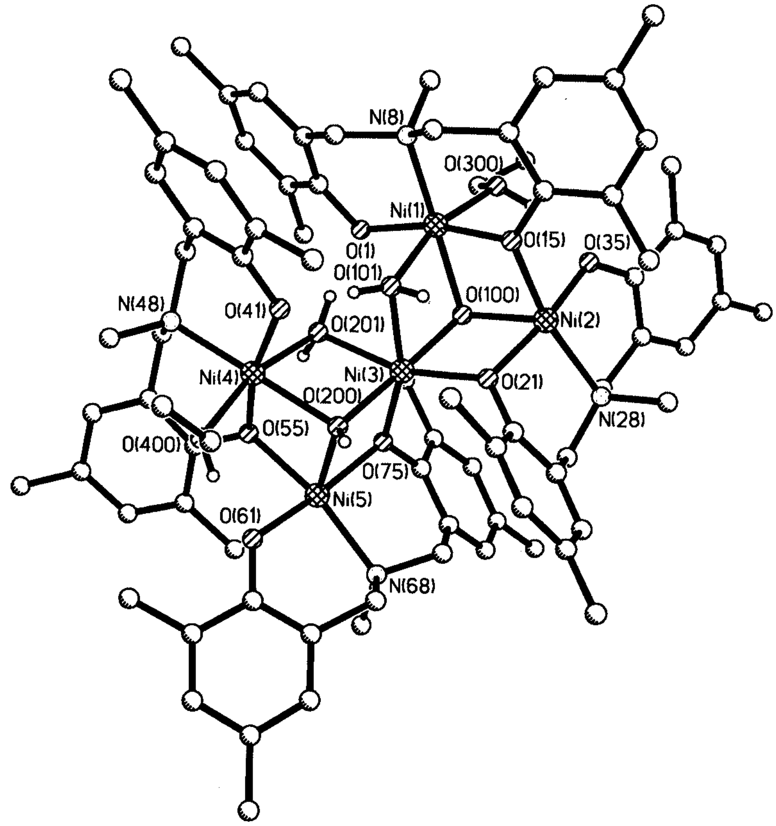

Figure 2. ORTEP representation of $[Ni_5L^N{}_4(\mu_3\text{-}OH)_2(\mu_2\text{-}OH_2)_2(EtOH)_2]$ (**3**)

The hydrogen atoms on the OH_2 and EtOH ligands enter into hydrogen bonding with the phenolate oxygens O(1), O(41), O(35) and O(61), with O(1)···O(201) 2.459 Å, O(41)···O(101) 2.448 Å, O(61)···O(400) 2.563 Å, and O(35)···O(300) 2.590 Å distances, thus presumably making the cluster unsusceptible to disruption. The central Ni(3) is six-coordinate, with oxygen donor atoms only. The long Ni···Ni distances (Table 2) exclude the possibility that the exchange coupling between the paramagnetic centres is transmitted directly through space. All Ni−O and Ni−N bond lengths are in conformity with the nickel ions in +II oxidation state.

Molecular Structure of 4

X-ray analysis reveals that **4** contains a Ni_6 unit and is best written as $[Ni_6L^N{}_4(\mu_2\text{-}OHMe)(\mu_3\text{-}OMe)_2(\mu_3\text{-}OH)_2(MeOH)_2(MeCN)_2]$, as shown in Figure 3(a). Figure 3(b) highlights the central hexanuclear core with the atom connectivity in the coordination sphere. Selected metrical parameters are given in Table 3. The structure of the Ni_6-cluster can be regarded as a face-shared distorted dicubane in which one of the corners of each cubane is missing. There is a twofold crystallographic axis passing through an oxygen atom (O60) of the bridging μ_2-methanol molecule. The nickel centres Ni(1) and Ni(1)# are five-coordinate, whereas Ni(2), Ni(3) and their symmetry related nickel centres are six-coordinate. Five-coordinated nickel centres possess square-pyramidal NO_4 geometries, with O(70) of the μ_3-OMe group as the axial ligand, whereas the six-coordinate nickel centres have NO_5 environments. The ancillary ligand $[L^N]^{2-}$, O(15), N(8) and O(1), together with the phenolate oxygen O(70) (which is a μ_2-bridging ligand) from a second ligand $[L^N]^{2-}$, form the equatorial plane for the five-coordinate Ni(1). The six-coordinate Ni(2) is bound to two μ_3-OH (O10 and O60), one μ_3-OMe (O70), one μ_2-OHMe (O60), one μ_2-phenolate (O1) and an acetonitrile (N50) ligand. On the other hand, Ni(3) is triply coordinated to the ligand $[L^N]^{2-}$ along with its monocoordination to a methanol (O80), a μ_3-hydroxide and a μ_3-methoxide group.

Magnetic Susceptibility Studies

Magnetic susceptibility data for polycrystalline samples of complexes **1**−**4** were collected in the 2−290 K temperature range in an applied magnetic field of 1 T to characterise the nature and magnitude of the exchange interaction propagated by the bridging ligands. We use the Heisenberg spin-Hamiltonian in the form $\hat{H} = -2J\,\hat{S}_A\cdot\hat{S}_B$ for an isotropic exchange coupling with $S_{Ni} = 1$ for **1**−**4**. The experimentally measured magnetic data were simulated by use of a least-squares fitting computer program[13] with a full-matrix diagonalisation of exchange coupling, Zeeman splitting, and axial single-ion zero-field interactions ($DS^2{}_z$), if necessary. The susceptibility data were corrected for diamagnetism (Pascal corrections). No temperature-independent paramagnetism (TIP) or paramagnetic impurities (PI) were used for the simulations. The experimental data are displayed in Figure 4 as the effective magnetic moment (μ_{eff})

Table 2. Selected interatomic distances [Å] and angles [deg] for $[Ni_5L^N{}_4(\mu_3\text{-}OH)_2(\mu_2\text{-}OH_2)_2(EtOH)_2]\cdot 0.75\ CH_2Cl_2$ (**3**)

Ni(1)–O(1)	1.999(3)	O(1)–Ni(1)–O(15)	167.33(14)
Ni(1)–O(15)	2.047(3)	O(1)–Ni(1)–O(300)	97.52(13)
Ni(1)–O(300)	2.081(3)	O(15)–Ni(1)–O(300)	91.05(13)
Ni(1)–N(8)	2.083(4)	O(1)–Ni(1)–N(8)	92.34(15)
Ni(1)–O(100)	2.096(3)	O(15)–Ni(1)–N(8)	96.20(14)
Ni(1)–O(101)	2.159(3)	O(300)–Ni(1)–N(8)	95.07(14)
Ni(2)–O(35)	1.980(3)	O(1)–Ni(1)–O(100)	89.11(13)
Ni(2)–O(100)	2.024(3)	O(15)–Ni(1)–O(100)	81.73(12)
Ni(2)–O(15)	2.031(3)	O(300)–Ni(1)–O(100)	88.70(13)
Ni(2)–O(21)	2.044(3)	N(8)–Ni(1)–O(100)	175.75(14)
Ni(2)–N(28)	2.100(4)	O(1)–Ni(1)–O(101)	92.62(12)
Ni(3)–O(100)	2.009(3)	O(15)–Ni(1)–O(101)	77.10(12)
Ni(3)–O(200)	2.011(3)	O(300)–Ni(1)–O(101)	164.01(13)
Ni(3)–O(75)	2.097(3)	N(8)–Ni(1)–O(101)	96.84(14)
Ni(3)–O(21)	2.102(3)	O(100)–Ni(1)–O(101)	79.10(12)
Ni(3)–O(201)	2.126(3)	O(35)–Ni(2)–O(100)	93.63(13)
Ni(3)–O(101)	2.128(3)	O(35)–Ni(2)–O(15)	89.06(13)
Ni(4)–O(41)	1.999(3)	O(100)–Ni(2)–O(15)	83.91(13)
Ni(4)–O(55)	2.059(3)	O(35)–Ni(2)–O(21)	172.21(14)
Ni(4)–O(400)	2.069(4)	O(100)–Ni(2)–O(21)	78.64(12)
Ni(4)–O(200)	2.085(3)	O(15)–Ni(2)–O(21)	89.22(13)
Ni(4)–N(48)	2.087(4)	O(35)–Ni(2)–N(28)	91.50(14)
Ni(4)–O(201)	2.187(3)	O(100)–Ni(2)–N(28)	112.41(14)
Ni(5)–O(61)	1.983(3)	O(15)–Ni(2)–N(28)	163.59(14)
Ni(5)–O(200)	2.030(3)	O(21)–Ni(2)–N(28)	92.29(14)
Ni(5)–O(55)	2.046(4)	O(100)–Ni(3)–O(200)	177.78(14)
Ni(5)–O(75)	2.053(3)	O(100)–Ni(3)–O(75)	103.80(13)
Ni(5)–N(68)	2.109(5)	O(200)–Ni(3)–O(75)	77.70(13)
		O(100)–Ni(3)–O(21)	77.62(12)
Ni(2)–O(15)–Ni(1)	96.78(13)	O(200)–Ni(3)–O(21)	103.18(13)
Ni(2)–O(21)–Ni(3)	99.91(13)	O(75)–Ni(3)–O(21)	117.96(13)
Ni(5)–O(55)–Ni(4)	95.99(14)	O(100)–Ni(3)–O(201)	96.66(13)
Ni(5)–O(75)–Ni(3)	100.09(13)	O(200)–Ni(3)–O(201)	81.87(13)
Ni(3)–O(100)–Ni(2)	103.83(14)	O(75)–Ni(3)–O(201)	82.63(13)
Ni(3)–O(100)–Ni(1)	100.30(13)	O(21)–Ni(3)–O(201)	159.34(13)
Ni(2)–O(100)–Ni(1)	95.43(13)	O(100)–Ni(3)–O(101)	81.81(13)
Ni(3)–O(101)–Ni(1)	94.66(13)	O(200)–Ni(3)–O(101)	96.27(13)
Ni(3)–O(200)–Ni(5)	103.88(14)	O(75)–Ni(3)–O(101)	161.52(13)
Ni(3)–O(200)–Ni(4)	100.99(15)	O(21)–Ni(3)–O(101)	80.32(12)
Ni(5)–O(200)–Ni(4)	95.67(13)	O(201)–Ni(3)–O(101)	79.21(13)
Ni(3)–O(201)–Ni(4)	94.22(13)	O(41)–Ni(4)–O(55)	166.40(13)
Ni(1)···Ni(2)	3.049(2)	O(41)–Ni(4)–O(400)	96.86(14)
Ni(1)···Ni(3)	3.152(2)	O(55)–Ni(4)–O(400)	93.35(14)
Ni(2)···Ni(3)	3.174(2)	O(41)–Ni(4)–O(200)	89.15(13)
Ni(3)···Ni(5)	3.181(2)	O(55)–Ni(4)–O(200)	82.01(13)
Ni(3)···Ni(4)	3.160(2)	O(400)–Ni(4)–O(200)	89.24(14)
Ni(4)···Ni(5)	3.050(2)	O(41)–Ni(4)–N(48)	92.99(16)
		O(55)–Ni(4)–N(48)	95.41(16)
		O(400)–Ni(4)–N(48)	93.11(15)
		O(200)–Ni(4)–N(48)	176.61(14)
		O(41)–Ni(4)–O(201)	92.13(13)
		O(55)–Ni(4)–O(201)	76.08(13)
		O(400)–Ni(4)–O(201)	164.92(15)
		O(200)–Ni(4)–O(201)	78.77(13)
		N(48)–Ni(4)–O(201)	98.52(14)
		O(61)–Ni(5)–O(200)	92.64(14)
		O(61)–Ni(5)–O(55)	88.17(15)
		O(200)–Ni(5)–O(55)	83.69(14)
		O(61)–Ni(5)–O(75)	170.92(15)
		O(200)–Ni(5)–O(75)	78.29(13)
		O(55)–Ni(5)–O(75)	90.77(13)
		O(61)–Ni(5)–N(68)	90.97(16)
		O(200)–Ni(5)–N(68)	114.27(15)
		O(55)–Ni(5)–N(68)	162.04(15)
		O(75)–Ni(5)–N(68)	92.80(15)

versus temperature (T). The solid lines in the figure represent the simulations.

The magnetic moment μ_{eff}/molecule for **1** and **2** of 6.54 μ_B ($\chi_M \cdot T = 5.332\ cm^3 \cdot K \cdot mol^{-1}$) and 6.52 μ_B ($\chi_M \cdot T = 5.233\ cm^3 \cdot K \cdot mol^{-1}$), respectively, at 290 K increases monotonically with decreasing temperature, reaching a maximum at 20 K with $\mu_{eff} = 7.54\ \mu_B$ ($\chi_M \cdot T = 7.115\ cm^3 \cdot K \cdot mol^{-1}$) for **1** and $\mu_{eff} = 7.15\ \mu_B$ ($\chi_M \cdot T = 6.444\ cm^3 \cdot K \cdot mol^{-1}$) for **2**. Below 20 K, μ_{eff} starts to decrease, reaching a value of 6.01 μ_B ($\chi_M \cdot T = 4.60\ cm^3 \cdot K \cdot mol^{-1}$) for **1** and 4.68 μ_B ($\chi_M \cdot T = 3.525\ cm^3 \cdot K \cdot mol^{-1}$) for **2** at 2 K (Figure 4); it is clear that the magnetic properties of **1** and **2** are dominated by a ferromagnetic exchange interaction between four $^3A_2$ nickel(II) ions as propagated by bridging methoxides. The structural parameters of **2** strongly suggest a lower symmetry than T_d (idealised D_{2d}) for the molecule. We have assumed the same symmetry for **1**.

The most important parameter in the magnetostructural correlation of the Ni_4O_4 cubane cores has been reported in the literature[4,9i,9h,9l,9p] to be the averaged Ni–O–Ni angle of a cubane face. In accordance with the three averaged Ni–O–Ni angles of 96.2°, 97.2°, and 101.3° observed for **2**, a three-J model based on the diagram shown in Scheme 2 was used to analyse the magnetic data for **1** and **2**.

Very good fits were obtained by use of this model, the best fit parameter sets being $J_1 = +2.39\ cm^{-1}$, $J_2 = -5.77\ cm^{-1}$, $J_3 = +6.9\ cm^{-1}$, $g = 2.27$ for **1** and $J_1 = +1.05\ cm^{-1}$, $J_2 = -4.1\ cm^{-1}$, $J_3 = +5.5\ cm^{-1}$, $g = 2.25$ for **2**. No zero-field splitting parameter D, TIP, or PI was needed to obtain the good quality of fit shown in Figure 4 as solid lines. The differences and natures of the signs of the exchange parameters are in full agreement with the Ni–O–Ni angle correlation and support the three-J model used, which takes account of the reduced symmetry of the cubane core observed in the X-ray structure of **2**. These results for **1** and **2** thus predict a switch from ferromagnetic to antiferromagnetic coupling only for Ni–O–Ni angles above ca. 98°, as also observed by us earlier.[4] We have also plotted the observed J values for **2** and other structurally characterised $[Ni_4(OR)_4]^{4+}$ cubanes against average Ni–O–Ni angles (Figure 5 and Table 4). The solid line in Figure 5, shown only as a guide for the eyes, allows us to see that the antiferromagnetic interactions ($-J$) fall fairly well on the correlated line with respect to Ni–O–Ni angles. In contrast, the positive J values scatter appreciably.

The magnetic data indicate that **1** and **2** have complicated, low-lying magnetic structures with non-diamagnetic ground states smaller than the spin state $S_t = 4$ expected for a ferromagnetically coupled tetranuclear nickel(II) species ($S_{Ni} = 1$). We have performed magnetisation measurements at applied magnetic fields of 1, 4, and 7 T and collected most of the magnetisation data in the 2–10 K temperature range (26 data point) and only 7 data points in the 12.3–260.0 K range, which are shown in Figure 6 as plots of M/Ngβ vs. βH/kT for **1** and **2**. It is clear from Figure 6 that the saturated magnetisation value reaches a value of approximately 3.45 for **1** and 3.10 for **2** in the 2.0–2.8 K temperature range at the highest field of 7 T. Noteworthy is

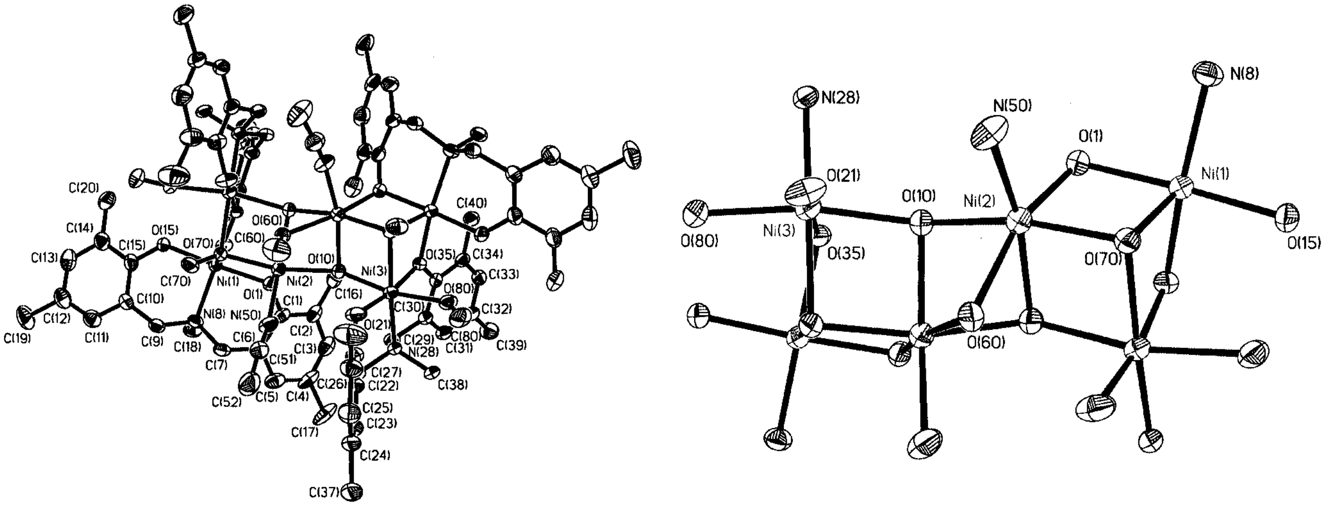

Figure 3. (a) Molecular structure of $[Ni_6L^N{}_4(\mu_2\text{-}OHMe)(\mu_3\text{-}OMe)_2(\mu_3\text{-}OH)_2(MeOH)_2(MeCN)_2]$ (**4**); (b) a view of **4** highlighting the coordination spheres of the hexanuclear nickel core

a downward tendency of magnetisation at low temperatures and low fields, presumably due to the population of the lower component of the multiplet split in the magnetic fields.

The nature of the field dependence of the susceptibility in the present system is extreme. The first-order Zeeman splitting of the ground state $S = 4$ results in nine separate energy levels. Thus, in the absence of zero-field splittings, the energy span of the ground state is 8gβH, so that at 1 T the ground state Zeeman levels span several wave numbers. It is not possible to calculate the ground state in the form of an S_t value; S is not a good quantum number to describe the ground state, but rather M_S. However, the magnetic analysis of **1** and **2** unambiguously demonstrates the overall ferromagnetic nature of the exchange interactions yielding "high-spin" ground states of $S_t > 3.0$.

The plot of μ_{eff} vs. T (Figure 4) for **3** shows the exchange coupling within the pentanuclear Ni^{II} complex to be predominantly ferromagnetic in nature. The effective magnetic moment μ_{eff} shows a maximum value of 8.52 μ_B ($\chi_M{\cdot}T$ = 9.079 $cm^3{\cdot}K{\cdot}mol^{-1}$) at 15 K and then decreases with decreasing temperature, reaching a value of 7.98 μ_B ($\chi_M{\cdot}T$ = 7.96 $cm^3{\cdot}K{\cdot}mol^{-1}$) at 5 K. The maximum μ_{eff} value of 8.52 μ_B clearly shows that both the five- and the six-coordinate nickel centres present in **3** are paramagnetic with $S_{Ni} = 1$. The maximum value of 8.52 μ_B is significantly smaller than the spin-only value of 10.95 μ_B expected for five ferromagnetically coupled Ni^{II} ions. The data were fitted by use of a two-J model based on the model shown in Scheme 3, as two different ranges of Ni−O−Ni angles of 94−96° and 100−103° prevail in **3**.

The spin-Hamiltonian used is

$$\hat{H} = -2J(\hat{S}_1{\cdot}\hat{S}_2 + \hat{S}_2{\cdot}\hat{S}_3 + \hat{S}_4{\cdot}\hat{S}_5 + \hat{S}_3{\cdot}\hat{S}_5) - 2J'(\hat{S}_1{\cdot}\hat{S}_3 + \hat{S}_3{\cdot}\hat{S}_4).$$

The best fit obtained with the parameter set $J' = +6.5$ cm^{-1}, $J = -0.24$ cm^{-1}, $g = 2.32$ is shown as a solid line in Figure 4. No zero-field splitting parameter D, TIP or PI was used to obtain the good quality of fit shown in Figure 4, suggesting that any zero-field splitting effects are small. As the value of J is very small, we checked its influence on the quality of the simulation by keeping $J = 0$ (fixed). The good quality of the simulation shown in Figure 4 could not be reproduced, indicating the importance, albeit very small, of J for the fit procedure. The spin ladder calculated by the evaluated exchange parameters exhibits clearly that the energy separation between low-lying states is very small (< 1 cm^{-1}), yielding an intermixing of the two states with $S_t = 4$ and $S_t = 5$. This is also corroborated with the magnetisation measurements at 1, 4, and 7 T, shown in Figure 6. The saturation behaviour observed at 7 T with a magnetisation value of ca. 4.5 unambiguously shows the dominant nature of the ferromagnetic coupling within the pentanuclear cluster, the nature of which is a mixture of $S_t = 4$ and $S_t = 5$ states.

Variable-temperature magnetic data for **4** (Figure 4) exhibit a steady decrease of μ_{eff} from 7.65 μ_B ($\chi_M{\cdot}T$ = 7.308 $cm^3{\cdot}K{\cdot}mol^{-1}$) at 290 K to 2.90 μ_B ($\chi_M{\cdot}T$ = 1.047 $cm^3{\cdot}K{\cdot}mol^{-1}$) at 2 K, which is indicative of an overall antiferromagnetic interaction within the hexanuclear nickel(II) complex **4**. That all five- and six-coordinate nickel(II) centres are paramagnetic with $S_{Ni} = 1$ is clearly attested to by the observed magnetic moment of μ_{eff} = 7.65 μ_B at 290 K. In accordance with the structural parameters, a three-J model, shown in Scheme 4, can be envisaged for the analysis of magnetic data.

The data were initially fit by use of g (fixed), J, J', and J'', which yielded a good fit (not shown) with $J = -1.16$ cm^{-1}, $J' = -9.11$ cm^{-1}, $J'' = -6.13$ cm^{-1}, $g = 2.269$ (fixed). To avoid overparametrisation, we did not use the zero-field splitting parameter D for the simulations. The above solution was discarded, as the Ni−O−Ni angles related to J'' are smaller than 90° and a small ferromagnetic coupling could be expected for the path. This suggested that a better fitting model should be used, so we again fitted the

Table 4. Selected bond lengths [Å] and angles [deg] for $[Ni_6L^N{}_4(\mu_2\text{-}OHMe)(\mu_3\text{-}OMe)_2(\mu_3\text{-}OH)_2(MeOH)_2(MeCN)_2]$ (**4**)

Ni(1)−O(15)	1.981(4)	Ni(1)−O(1)	2.017(4)
Ni(1)−O(35)#1[a]	2.030(4)	Ni(1)−O(70)	2.031(4)
Ni(1)−N(8)	2.121(5)	Ni(2)−O(10)	2.028(4)
Ni(2)−O(70)	2.031(4)	Ni(2)−O(1)	2.054(4)
Ni(2)−O(10)#1	2.073(4)	Ni(2)−N(50)	2.086(6)
Ni(2)−O(60)#1	2.224(9)	Ni(2)−O(60)	2.233(8)
Ni(3)−O(21)	1.989(4)	Ni(3)−O(35)	2.038(4)
Ni(3)−O(80)	2.075(5)	Ni(3)−O(10)	2.097(4)
Ni(3)−N(28)	2.101(5)	Ni(3)−O(70)#1	2.140(4)
O(15)−Ni(1)−O(1)	177.20(16)	O(15)−Ni(1)−O(35)#1	88.84(15)
O(1)−Ni(1)−O(35)#1	88.39(15)	O(15)−Ni(1)−O(70)	97.86(17)
O(1)−Ni(1)−O(70)	81.38(16)	O(35)#1−Ni(1)−O(70)	83.45(15)
O(15)−Ni(1)−N(8)	90.54(18)	O(1)−Ni(1)−N(8)	92.25(17)
O(35)#1−Ni(1)−N(8)	165.41(18)	O(70)−Ni(1)−N(8)	111.06(18)
O(10)−Ni(2)−O(70)	167.39(16)	O(10)−Ni(2)−O(1)	100.19(16)
O(70)−Ni(2)−O(1)	80.50(15)	O(10)−Ni(2)−O(10)#1	82.67(18)
O(70)−Ni(2)−O(10)#1	84.75(15)	O(1)−Ni(2)−O(10)#1	96.87(17)
O(10)−Ni(2)−N(50)	96.33(19)	O(70)−Ni(2)−N(50)	95.86(19)
O(1)−Ni(2)−N(50)	101.39(19)	O(10)#1−Ni(2)−N(50)	161.6(2)
O(10)−Ni(2)−O(60)	86.0(2)	O(70)−Ni(2)−O(60)	90.3(2)
O(1)−Ni(2)−O(60)	164.1(2)	O(10)#1−Ni(2)−O(60)	69.2(2)
N(50)−Ni(2)−O(60)	92.4(3)		
O(21)−Ni(3)−O(35)	171.31(16)	O(21)−Ni(3)−O(80)	96.2(2)
O(35)−Ni(3)−O(80)	87.87(18)	O(21)−Ni(3)−O(10)	91.09(18)
O(35)−Ni(3)−O(10)	83.68(16)	O(80)−Ni(3)−O(10)	168.10(17)
O(21)−Ni(3)−N(28)	94.36(18)	O(35)−Ni(3)−N(28)	93.27(18)
O(80)−Ni(3)−N(28)	90.36(18)	O(21)−Ni(3)−O(70)#1	91.79(16)
O(35)−Ni(3)−O(70)#1	80.60(15)	O(80)−Ni(3)−O(70)#1	88.86(16)
O(10)−Ni(3)−O(70)#1	81.52(15)	N(28)−Ni(3)−O(70)#1	173.85(18)
N(28)−Ni(3)−O(10)	98.46(17)		
Ni(1)−O(70)−Ni(3)#1	94.93(16)	Ni(2)−O(70)−Ni(3)#1	96.80(15)
Ni(2)−O(70)−Ni(1)	99.07(17)	Ni(2)#1−O(60)−Ni(2)	78.6(3)
Ni(1)#1−O(35)−Ni(3)	98.20(17)	Ni(1)−O(1)−Ni(2)	98.76(17)
Ni(2)#1−O(10)−Ni(3)	96.85(17)	Ni(2)−O(10)−Ni(3)	144.5(2)
Ni(2)−O(10)−Ni(2)#1	86.98(16)		
Ni(1)···Ni(2)	3.091(2)		
Ni(2)···Ni(3)	3.929(2)		
Ni(2)···Ni(2)#1	2.823(2)		
Ni(2)···Ni(3)#1	3.119(2)		
Ni(1)···Ni(3)#1	3.074(2)		

[a] #1 indicates the symmetry-related atom.

data with use of three different exchange parameters, but with the following constraints: g, J, and J' free for reiteration but J'' fixed between zero and a small positive value of +2.0. The quality of fit became poor, but the exchange values vary negligibly between −1.79 and −1.95 cm^{-1} for J and between −9.0 and −8.93 cm^{-1} for J', indicating that although J'' has some influence on the quality of fit, J and J' are nearly independent of J''. We therefore started another simulation, making all four parameters free to move. The quality of fit increased dramatically, yielding the following parameters: $g = 2.295$, $J = -1.15$ cm^{-1}, $J' = -9.87$ cm^{-1}, and $J'' = -9.66$ cm^{-1}. As the evaluated values for J' and J'' are nearly the same, we carried out the magnetic analysis with the constraint $J' = J''$ (i.e., a two-J model to reduce the number of fit parameters). A very good fit obtained with the parameter set $g = 2.295$, $J = -1.12$ cm^{-1} and $J' = J'' = -9.77$ cm^{-1} is shown as a solid line in Figure 4. We note that the sign of the exchange parameter J'' is not in line with the commonly accepted Ni−O−Ni angle correlation; this might be due to three different competitive exchange couplings operating on Ni(2) and Ni(2)* making the correlation more complex. Irrespective of that, the two-J model suitably describes the magnetic properties of complex **4**, which does not possess a well separated ground state of $S_t = 0$, as would be expected for an antiferromagnetically coupled hexanuclear Ni^{II} complex; the excited state of $S_t = 1$ is energetically very close to the ground state, and so a non-zero magnetic moment is observed even at 2 K. This is also corroborated by the variable-temperature magnetisation curves at 1, 4, and 7 T (Figure 6).

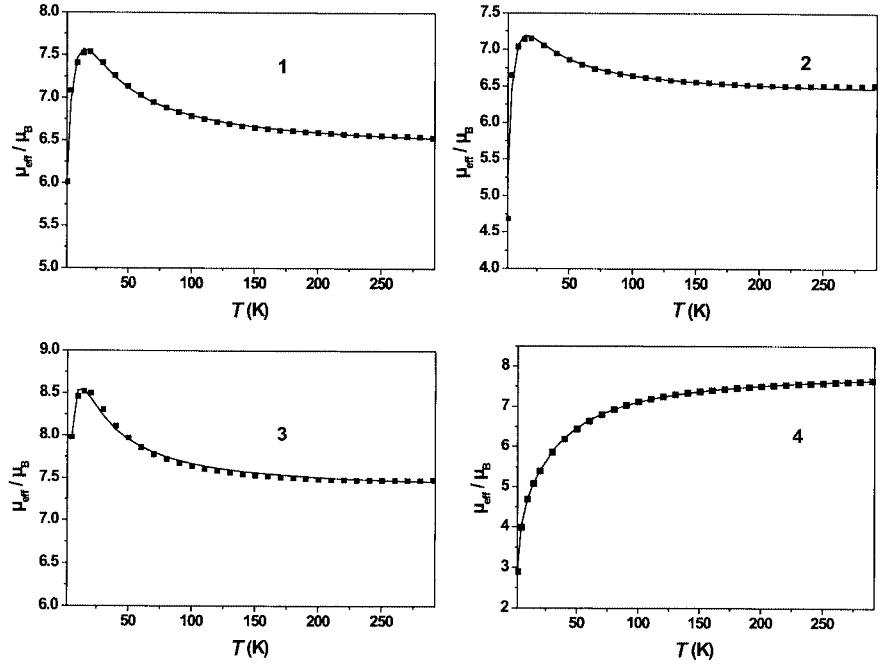

Figure 4. Plots of μ_{eff} vs. T for solid **1**−**4**; the solid lines represent the best fit of the data to the exchange coupling model

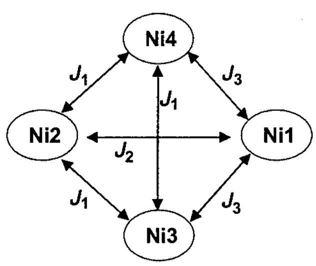

Scheme 2

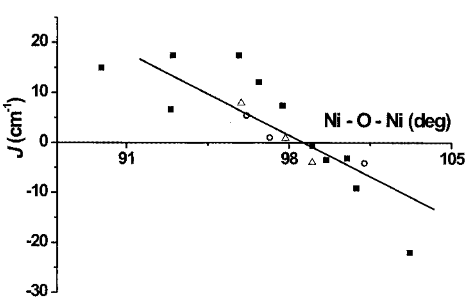

Figure 5. A plot of average Ni−O−Ni angles vs. the exchange interactions (*J*); filled squares are literature data, triangles are from ref.[4] and open circles are from this work; the solid line is drawn only as a guide

Concluding Remarks

The tridentate bisphenol ligands used in this work give rise to polynuclear nickel(II) complexes of different nuclearity: four, five or six, depending on the heterodonor atoms such as S, Se, or N. The S- and Se-containing ligands H_2L^S and H_2L^{Se} coordinate facially with five-membered chelation to a metal centre, whereas the N-containing ligand H_2L^N forms six-membered chelate rings and, presumably as a consequence of the ring size, the ligand H_2L^N coordinates meridionally. This different geometrical coordination mode seems to yield tetranuclear complexes with H_2L^S and H_2L^{Se}, but H_2L^N results in penta- and hexanuclear complexes. Thus, our starting goal of preparing polynuclear complexes with ferromagnetic exchange coupling has been partly achieved, although the hexanuclear nickel(II) complex does not belong to the class of molecules with large spin ground states.

Complexes **1** and **2** exhibit overall ferromagnetic interactions, producing ground states with "large spins". The *J* values obtained here are similar to those found for other $[Ni_4(\mu_3\text{-}OR)_4]^{4+}$ cubanes reported in the literature[9] (Table 4). The coupling between the nickel(II) ions is very close to the crossover point between antiferromagnetic and ferromagnetic coupling. In all cases, bond angles of less than ca. 98° produce ferromagnetic coupling, whilst those that are larger give rise to antiferromagnetic coupling. This correlation is similar to that in the bridged Cu−O−Cu systems,[14] in which ferromagnetic pathways of the form[15] $e_g \perp O \perp e_g$ are found to be most effective for Cu−O−Cu angles smaller than 97.5°.

Complex **2** contains the low-symmetry cubane core $[Ni_4(\mu_3\text{-methoxide})_4]^{4+}$ with differing Ni···Ni distances and Ni−O−Ni angles, resulting in three types of Ni_2O_2 faces. The observation of three discrete exchange parameters for **2** is consistent with the lower symmetry of the cubane; the symmetry of **2** is lower than that in the majority of the nickel-cubanes reported in the literature. Figure 5 shows a plot of *J* vs. Ni−O−Ni angles for all structurally characterised Ni_4O_4 cubane cores, irrespective of their symmetry; it exhibits a large variation of *J* values within a small span of Ni−O−Ni angles (90−103°). This figure also indicates that

Table 5. J as a function of the Ni−O−Ni angles for the $[Ni_4(\mu_3\text{-}OR)_4]$ cubanes

Complex[a]	Ni−O−Ni$_{av}$ (deg)	J (cm^{-1})	Reference
$[Ni_4(\mu_3\text{-}OMe)_4(sal)_4(EtOH)_4]$	97.73	7.46	[9a,9b]
$[Ni_4(\mu_3\text{-}OH)_4(chta)_4(NO_3)_4]$	99.0	−0.57	[9c,9h]
$[Ni_4(\mu_3\text{-}OMe)_4(TMB)_4(\mu\text{-}O_2CMe)_4]$	93.0 100.9	17.5	[9e]
$[Ni_4(\mu_3\text{-}OH)_4(tzdt)_4(py)_4]$	95.89 103.2	17.5	[9i]
$[Ni_4(\mu_3\text{-}OMe)_4(dbm)_4(MeOH)_4]$	96.7 99.6	2.2	[9l]
$[Ni_4(\mu_3\text{-}OH)_2(pypentO)(pym)\text{-}(\mu\text{-}OAc)_2(NCS)_2(OH_2)]$	89.9 92.9 100.5	15.0 6.7 −3.09	[9p]
$[Ni_4(\mu_3\text{-}OMe)_2(LH)_2(OAc)_2(MeOH)_2]$	95.94 97.85 99.0	8.0 1.0 −3.8	[4]
$[Ni_4(\mu_3\text{-}OMe)_4(L^{Se})_2(MeOH)_2(MeCN)_2]$	96.17 97.17 101.25	5.50 1.05 −4.1	this work this work this work

[a] salH = salicylaldehyde; chta = *r*-1-*c*-3-*c*-5 triaminocyclohexane; TMB = 2,5-dimethyl-2,5-diisocyanohexane; dzdt = 1,3-thiazolidine-2-thione; dbmH = dibenzoylmethane; py = pyridine; pypentO = 1,5-bis[2-pyridylmethyl)amino]-3-pentanolate; pym = 2-pyridylmethoxide; L = a dinucleating Schiff-base ligand.

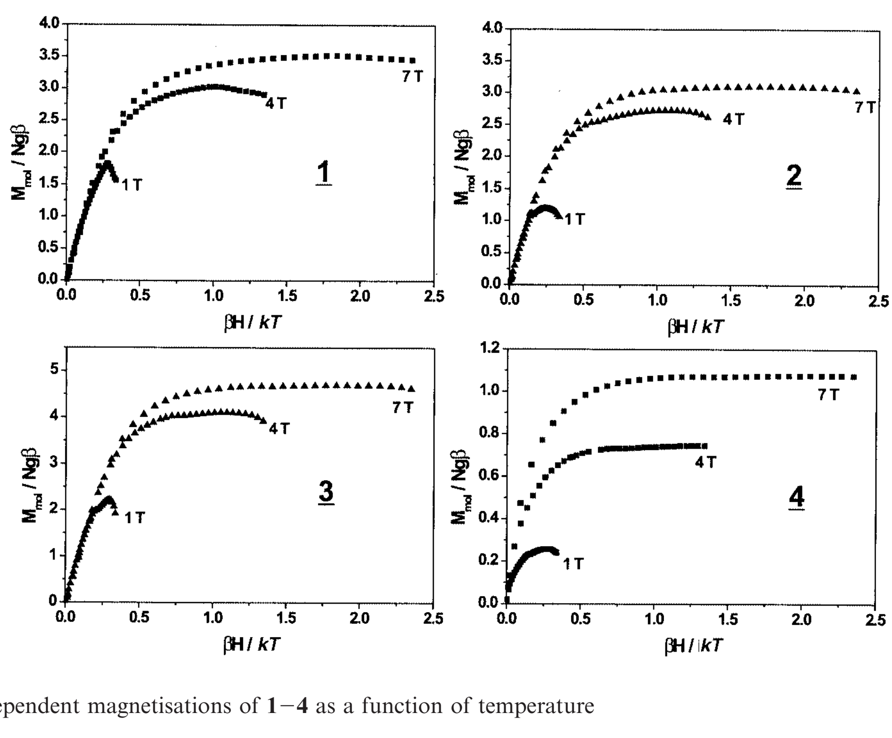

Figure 6. The field-dependent magnetisations of **1−4** as a function of temperature

the symmetry of the cubane core has a profound effect on the magnetostructural correlation. In particular, the scattering of the positive J values is noteworthy. This is not surprising in view of the high tolerance attached in general to the positive J values (ferromagnetic interactions) evaluated through simulation of the susceptibility data. The syn-

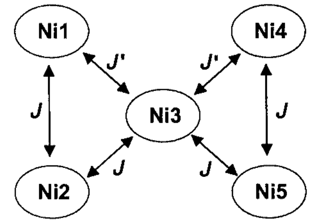

Scheme 3

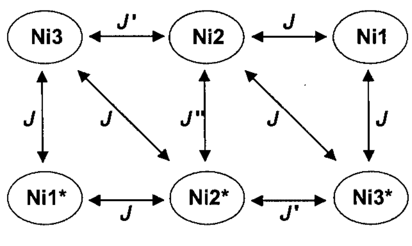

Scheme 4

thesis of more such distorted cubane-type Ni^{II} complexes would therefore be warranted in order to resolve this problem of magnetostructural correlation.

In the literature, there are only two examples of pentanuclear Ni^{II} complexes in which all five metal centres are paramagnetic with $S_{Ni} = 1$. The first example, $[Ni_5(en)_4(\mu_3\text{-}OH)_2(NO_2)_8]$,[10g] reported as early as 1981, contains a planar, pentameric arrangement of nickel(II) ions, linked by bridging hydroxide and nitrite ligands; unfortunately no magnetic data were reported. In the second example,[10a] four six-coordinate Ni^{II} ions are arranged at the apices of a tetrahedron with the fifth nickel at the centre; the compound is antiferromagnetically coupled with an admixed ground state of $S_t = 0, 1$. *Complex* **3** *constitutes the first example of a pentanuclear* Ni^{II} *complex exhibiting ferromagnetic interactions with an intermixed ground state of* $S_t = 5.0$ *and 4.0.* Pentanuclear nickel(II) complexes with five $S_{Ni} = 1$ centres still belong to the rare examples of coordination complexes.

An apparently trivial modification of the reaction, use of a mixed solvent medium, resulted in the isolation of complex **4**, a hexanuclear Ni^{II} complex, under reaction conditions otherwise the same as those used for complex **3**. The amount of water present in the reaction mixture is decisive for the isolation of complex **4**. The central nickel centres, Ni(2) and Ni(2)#, are primarily devoid of coordination to the ancillary ligand $[L^N]^{2-}$. In complex **4**, and also in **3**, the ligand $[L^N]^{2-}$ also for the first time shows the bridging functionality through one of its phenolate oxygens. The magnetic studies exhibiting predominantly antiferromagnetic exchange between the metal centres are disappointing in view of the original expectation of large-spin ground states. A simple two-J model shows good agreement with experimentally ascertained low-temperature magnetic data. The sign of an exchange coupling parameter J'' ($-9.77\ cm^{-1}$) cannot be correlated with the corresponding Ni−O−Ni angles, which are appreciably smaller than 90°.

Experimental Section

Materials and Physical Measurements: Commercial grade chemicals were used for synthetic purposes, and solvents were distilled and dried before use. Fourier transform infrared spectroscopy on KBr pellets was performed on a Perkin−Elmer 2000 FT-IR instrument. Solution electronic spectra were measured on a Perkin−Elmer Lambda 19 spectrophotometer. Mass spectra were recorded either in the EI or the ESI (in CH_2Cl_2) modes with a Finnigan MAT 95 or 8200 spectrometer. Magnetic susceptibilities of the polycrystalline samples were recorded on a SQUID magnetometer (MPMS, Quantum Design) in the 2−290 K temperature range, with an applied field of 1 T. Diamagnetic contributions were estimated for each compound by use of Pascal's constants.

X-ray Crystallographic Data Collection and Refinement of the Structures: Single crystals of **2**, **3**, and **4** were coated with perfluoropolyether, picked up with glass fibres, and mounted on a Nonius Kappa-CCD diffractometer equipped with a cryogenic nitrogen cold stream operating at 100(2) K. Graphite monochromated Mo-K_α radiation ($\lambda = 0.71073$ Å) was used. Intensity data were corrected for Lorentz and polarisation effects. The intensity data set of **2** and **3**, were corrected for absorption by use of the program Gaussian face-indexed, whereas that of **4** was not corrected. The Siemens SHELXTL software package (G. M. Sheldrick, Universität Göttingen) was used for solution, refinement, and depiction of the structure, and neutral atom scattering factors of the program were used. All structures were solved and refined by direct methods and difference Fourier techniques. Non-hydrogen atoms were refined anisotropically, and hydrogen atoms were placed at calculated positions and refined as riding atoms with isotropic displacement parameters. Details of the data collection and structure refinements are summarised in Table 5.

CCDC-204445 (**2**), -204446 (**3**), and -204447 (**4**) contain the supplementary crystallographic data for this paper. These data can be obtained free of charge at www.ccdc.cam.ac.uk/conts/retrieving.html [or from the Cambridge Crystallographic Data Centre, 12, Union Road, Cambridge CB2 1EZ, UK; Fax: (internat.) +44-1223/336-033; E-mail: deposit@ccdc.cam.ac.uk].

Ligand Synthesis: The ligands H_2L^S [16] and H_2L^N [3,17] were synthesised by the published procedures. The ligand H_2L^{Se} was synthesised by a modification of the method described in the literature.[18]

2,2′-Selenobis(4,6-di-*tert*-butylphenol) (H_2L^{Se}): A suspension of 2,4-di-*tert*-butylphenol (61.89 g, 0.3 mol) and SeO_2 (11.1 g, 0.1 mol) in conc. HCl (55 mL) was heated at 80 °C with constant stirring for 2 h. The mixture was then cooled, extracted with $CHCl_3$ (3 × 100 mL), washed with brine solution (2 × 50 mL) and then with water (100 mL), dried with Na_2SO_4 and concentrated in vacuo. The crude brown product was then recrystallised from heptane and MeOH (1:1) to obtain a pure white compound. Yield: 18.5 g (25%). Melting Point: 141 °C. $C_{28}H_{42}SeO_2$ (489.6 g/mol): calcd. C 68.69, H 8.65; found C, 68.7, H 8.7%. ^1H NMR ($CDCl_3$): δ = 1.20 (s, 18 H); 1.38 (s, 18 H); 6.25 (s, OH, 2 H); 7.24 (m, 4 H) ppm. ^{13}C NMR ($CDCl_3$): δ = 29.5 (s, *tert*-butyl); 31.6 (s, *tert*-butyl); 34.3 (s, *tert*-butyl); 35.2 (s, *tert*-butyl); 117.0 (s), 125.4 (s); 129.6 (s); 135.7 (s); 143.3 (s), and 151.6 (s) ppm. MS (EI): The desired molecular ion ($M^+ = 490$) was observed in the ratio calculated for the naturally abundant isotope mixture of Se-74, 76, 77, 80, and 82.

General Method of Synthesis for Complexes 1 and 2: The ligand (1 mmol) was dissolved in a mixture of MeOH (12.5 mL) and

Table 5. Crystallographic data for $[Ni_4L^{Se}_2(\mu_3\text{-}OMe)_4(MeOH)_4(MeCN)_2]\cdot 3.5MeCN\cdot 0.5MeOH$ (**2**), $[Ni_5L^N_4(\mu_3\text{-}OH)_2(\mu_2\text{-}OH_2)_2(EtOH)_2]\cdot 0.75CH_2Cl_2$ (**3**), and $[Ni_6L^N_4(\mu_2\text{-}OHMe)(\mu_3\text{-}OMe)_2(\mu_3\text{-}OH)_2(HOMe)_2(MeCN)_2]$ (**4**)

	Ni^{II}_4 **2**	Ni^{II}_5 **3**	Ni^{II}_6 **4**
Empirical formula	$C_{68}H_{114}N_2Ni_4O_{12}Se_2\cdot 3.5CH_3CN\cdot 0.5CH_3OH$	$C_{80}H_{110}N_4Ni_5O_{14}\cdot 0.75CH_2Cl_2$	$C_{85}H_{118}N_6Ni_6O_{15}$
Molecular mass	1704.08	1708.96	1816.11
Temperature	100(2) K	100(2) K	100(2) K
Wavelength (Mo-K_α)	0.71073 Å	0.71073 Å	0.71073 Å
Crystal system	Triclinic	Monoclinic	Monoclinic
Space group	$\bar{P}$	$P2_1/c$	$C2/c$
Unit cell dimensions	a = 15.4538(6) Å b = 16.6106(8) Å c = 18.2370(10) Å α = 90.31(1)° β = 108.99(1)° γ = 105.71(1)°	a = 20.6988(8) Å b = 25.7220(8) Å c = 17.8131(6) Å β = 111.65(1)°	a = 20.6998(12) Å b = 15.0379(9) Å c = 28.599(2) Å β = 110.98(1)°
Volume [Å^3]; Z	4238.7(4); 2	8814.9(5); 4	8312.2(9); 4
Density (calcd.) [Mg/m^3]	1.335	1.288	1.451
Absorption coefficient [mm^{-1}]	1.791	1.153	1.399
F(000)	1796	3606	3832
Crystal size [mm]	0.26 × 0.25 × 0.11	0.19 × 0.14 × 0.13	0.07 × 0.04 × 0.04
θ range for data collect.	4.09 to 28.50°	2.92 to 23.00°	2.11 to 24.00°
Reflections collected	96465	62882	20329
Independent reflect.	21433 [R(int.) = 0.0802]	12227 [R(int.) = 0.0938]	[6529 [R(int.) = 0.0694]
Absorption correction	Gaussian, face indexed	Gaussian, face indexed	not corrected
Data/restraints/param.	21321/150/873	12227/36/1030	6529/0/519
Goodness-of-fit on F^2	1.031	1.056	1.016
Final R indices [$I > 2\sigma(I)$]	R_1 = 0.0538; wR_2 = 0.1277	R_1 = 0.0509; wR_2 = 0.1287	R_1 = 0.0587; wR_2 = 0.1193
R indices (all data)	R_1 = 0.0851; wR_2 = 0.1441	R_1 = 0.0710; wR_2 = 0.1416	R_1 = 0.1069; wR_2 = 0.1402

MeCN (2.5 mL). LiOMe (1 M methanolic solution, 2 mL, 2 mmol) was added, and the solution was stirred for 5 min. $NiCl_2\cdot 6H_2O$ (0.24 g, 1 mol) was added to that yellow solution, and the resulting green solution was stirred for 5 min and then kept for slow evaporation of solvent under air. A green crystalline compound separated overnight.

$[Ni_4L^S_2(\mu\text{-}OMe)_4(MeOH)_4(MeCN)_2]$ (1): Yield: 0.42 g (58%). $C_{68}H_{114}S_2O_{12}Ni_4N_2$ (1450.54): calcd. C 56.31, H 7.92, S 4.42, N 1.93, Ni 16.18; found C 55.7, H 7.9, S 4.3, N 2.0, Ni 15.7%. IR: $\tilde{\nu}$ = 3423 cm^{-1} (br), 2957−2818 (s), 2315−2253, 1432 (s), 1298 (s), 1047 (s), 829, 731.

$[Ni_4L^{Se}_2(\mu\text{-}OMe)_4(MeOH)_4(MeCN)_2]$ (2): Yield: 0.34 g (44%). $C_{68}H_{114}Se_2O_{12}Ni_4N_2$ (1544.34): calcd. C 52.89, H 7.44, Ni 15.20; found C 49.6, H 7.3, Ni 14.9%. IR: $\tilde{\nu}$ = 3404 cm^{-1} (br), 2954−2821 (s), 2315−2253, 1429 (s), 12989 (s), 1047 (s), 828, 724.

$[Ni_5L^N_4(\mu_3\text{-}OH)_2(\mu\text{-}H_2O)_2(EtOH)_2]\cdot 0.75CH_2Cl_2$ (3): The ligand (1 mmol, 0.30 g) was dissolved in EtOH (15 mL). LiOEt (1 M methanolic solution, 2 mL, 2 mmol) was added, and the solution was stirred for 5 min. $NiCl_2\cdot 6H_2O$ (0.24 g, 1 mol) was added to the yellow solution, and the resulting light green solution was stirred under air. The separated yellowish green microcrystalline compound was filtered and dried. X-ray-quality crystals were grown from a solvent mixture (1:2) of CH_2Cl_2 and EtOH. Yield: 0.32 g (75%). $C_{80}H_{140}N_4O_{14}Ni_5\cdot 0.75CH_2Cl_2$ (1708.96): calcd. C 56.75, H 6.58, N 3.28, Ni 17.17; found C 56.9, H 6.7, N 3.2, Ni 17.4. IR: $\tilde{\nu}$ = 3510 cm^{-1} (br), 2915 (s), 1477 (s), 1263 (s), 1162, 801, 648, 451.

$[Ni_6L^N_4(\mu\text{-}MeOH)(\mu_3\text{-}OMe)_2(\mu_3\text{-}OH)_2(MeOH)_2(MeCN)_2]$ (4): The ligand (0.5 mmol, 0.15 g) was treated with NaOMe (2 mL, 0.5 M methanolic solution) in a solvent mixture of MeCN (3 mL) and MeOH (15 mL). $NiCl_2\cdot 6H_2O$ (0.12 g, 0.5 mmol) was added, and the light green solution was kept at room temperature. A green crystalline complex separated out overnight. Yield: 0.11 g (49%). $C_{85}H_{118}N_6O_{15}Ni_6$ (1816.04): calcd. C 56.22, H 6.55, N 4.63, Ni 19.39; found C 53.3, H 6.3, N 3.9, Ni 19.2. IR: $\tilde{\nu}$ = 3448 cm^{-1} (br), 2918 (s), 1475 (s), 1266 (s), 1057, 802, 453.

Acknowledgments

Financial support from the DFG, the Max-Planck Society and Fonds der Chemischen Industrie is gratefully acknowledged. Thanks are due to Mrs. H. Schucht, Mrs. R. Wagner, and Mr. A. Göbels for skilful technical assistance.

[1] For selected examples see: [1a] L. Que Jr., W. Tolman, *Angew. Chem.* **2002**, *114*, 1160; *Angew. Chem. Int. Ed.* **2002**, *41*, 1114. [1b] V. Mahadevan, R. J. M. Klein Gebbink, T. D. P. Stack, *Cur. Opin. Chem. Biol.* **2000**, *4*, 228. [1c] J. Du Bois, T. J. Mizoguchi, S. J. Lippard, *Coord. Chem. Rev.* **2000**, 200−202, 443. [1d] *Multicopper Oxidases* (Ed.: A. Messerschmidt), World Scientific, Singapore, **1997**. [1e] *Bioinorganic Chemistry of Copper* (Eds.: K. D. Karlin, Z. Tyeklar), Chapman & Hall, New York, **1993**.

[2] See for example: [2a] "*Journal of Solid State Chemistry*", Vol. 159, No. 2, July **2001** − a tribute to Olivier Kahn. [2b] *Magnetic Molecular Materials* (Eds.: D. Gatteschi, O. Kahn, J. S. Miller, F. Palacio), Kluwer, Dordrecht, The Netherlands, **1991**.

[3] T. Weyhermüller, T. K. Paine, E. Bothe, E. Bill, P. Chaudhuri, *Inorg. Chim. Acta* **2002**, *337*, 344.

[4] S. Mukherjee, T. Weyhermüller, E. Bothe, K. Wieghardt, P. Chaudhuri, *Eur. J. Inorg. Chem.* **2003**, 863.

[5] S. Mukherjee, T. Weyhermüller, E. Bothe, P. Chaudhuri, *Eur. J. Inorg. Chem.* **2003**, 1956.

[6] R. Siefert, T. Weyhermüller, P. Chaudhuri, *J. Chem. Soc., Dalton Trans.* **2000**, 4656.

[7] V. V. Pavlishchuk, F. Birkelbach, T. Weyhermüller, K. Wieghardt, P. Chaudhuri, *Inorg. Chem.* **2002**, *41*, 4405.

[8] Selected examples: [8a] K. S. Murray, *Adv. Inorg. Chem.* **1995**, *43*, 261. [8b] V. V. Pavlishchuk, S. V. Kolotilov, A. W. Addison, M. J. Prushan, D. Schollmeyer, L. K. Thompson, E. A. Goreshnik, *Angew. Chem. Int. Ed.* **2001**, *40*, 4734. [8c] J. M. Cle-

mente-Juan, H. Andres, J. J. Borrás-Almenar, E. Coronado, H. U. Güdel, M. Eebersold, G. Kearly, H. Büttner, M. Zolliker, *J. Am. Chem. Soc.* **1999**, *121*, 10021. [8d] A. Escuer, R. Vincente, S. B. Kumar, F. A. Mautner, *J. Chem. Soc., Dalton Trans.* **1998**, 3473. [8e] H. Adams, S. Clunas, D. E. Fenton, *Chem. Commun.* **2002**, 418. [8f] M. Du, X.-H. Bu, Y.-M. Guo, L. Zhang, D.-Z. Liao, J. Ribas, *Chem. Commun.* **2002**, 1478. [8g] T. K. Karmakar, S. K. Chandra, J. Ribas, G. Mostafa, T. H. Lu, B. K. Ghosh, *Chem. Commun.* **2002**, 2364.

[9] [9a] J. E. Andrew, A. B. Blake, *J. Chem. Soc., A* **1969**, 1456. [9b] J. A. Barnes, W. E. Hatfield, *Inorg. Chem.* **1971**, *10*, 2355. [9c] B. Aurivillius, *Acta Chem. Scand., Ser. A* **1977**, *31*, 501. [9d] J. A. Bertrand, C. Marabella, D. G. Vanderveer, *Inorg. Chim. Acta* **1978**, *26*, 113. [9e] W. L. Gladfelter, M. W. Lynch, W. P. Schaefer, D. N. Hendrickson, H. B. Grey, *Inorg. Chem.* **1981**, *20*, 2390. [9f] F. Paap, E. Bouwman, W. L. Driessen, R. A. G. de Graaf, J. Reedijk, *J. Chem. Soc., Dalton Trans.* **1985**, 737. [9g] K. Bizilj, S. G. Hardin, B. F. Hoskins, P. J. Oliver, E. R. T. Tiekink, G. Winter, *Aust. J. Chem.* **1986**, *39*, 1035. [9h] P. D. Boyd, R. L. Martin, G. Schwarzenbach, *Aust. J. Chem.* **1988**, *41*, 1449. [9i] L. Ballester, E. Coronado, A. Gutiérrez, A. Monge, M. F. Perpinán, E. Pinilla, T. Rico, *Inorg. Chem.* **1992**, *31*, 2053. [9j] A. J. Atkins, A. J. Blake, M. Schröder, *J. Chem. Soc., Chem. Commun.* **1993**, 1662. [9k] A. J. Blake, E. K. Brechin, A. Codron, R. O. Gould, C. M. Grant, S. Parsons, J. M. Rawson, R. E. P. Winpenny, *J. Chem. Soc., Chem. Commun.* **1995**, 1983. [9l] M. A. Halcrow, J.-S. Sun, J. C. Huffman, G. Christou, *Inorg. Chem.* **1995**, *34*, 4167. [9m] M. S. E. Fallah, E. Rentschler, A. Caneschi, D. Gatteschi, *Inorg. Chim. Acta* **1996**, *247*, 231. [9n] A. Escuer, M. Font-Bardiá, S. B. Kumar, X. Solans, R. Vicente, *Polyhedron* **1999**, *18*, 909. [9o] M. L. Tong, H. K. Lee, S.-L. Zheng, X.-M. Chen, *Chem. Lett.* **1999**, 1087. [9p] J. M. Clemente-Juan, B. Chansou, B. Donnadieu, J.-P. Tuchagues, *Inorg. Chem.* **2000**, *39*, 5515.

[10] [10a] V. Tangoulis, C. P. Raptopoulou, A. Terzis, E. G. Bakalbassis, E. Diamantopoulou, S. P. Perlepes, *Inorg. Chem.* **1998**, *37*, 3142. [10b] S.-J. Shieh, C.-C. Chou, G.-H. Lee, C.-C. Wang, S.-M. Peng, *Angew. Chem. Int. Ed. Engl.* **1997**, *36*, 56. [10c] C. S. Velazquez, T. F. Baumann, M. M. Olmsted, H. Hope, A. G. Barrett, B. M. Hoffman, *J. Am. Chem. Soc.* **1993**, *115*, 9997. [10d] D. Fenske, H. Krautscheid, M. Müller, *Angew. Chem. Int. Ed. Engl.* **1992**, *31*, 321. [10e] B. K. Koo, E. Block, H. Kang, S. Liu, J. Jubieta, *Polyhedron* **1988**, *7*, 1397. [10f] M. Knege, G. Henkel, *Z. Naturforsch., Teil B* **1987**, *42*, 1121. [10g] A. J. Finney, M. A. Hitchman, C. L. Raston, G. L. Rowbottom, A. H. White, *Aust. J. Chem.* **1981**, *34*, 2139. [10h] F. Cecconi, C. A. Ghilardi, S. Midollini, A. Orlandini, A. Vacca, *Inorg. Chem. Commun.* **2000**, *3*, 276. [10i] C-Y. Yeh, Y. L. Chiang, G.-H. Lee, S.-M. Peng, *Inorg. Chem.* **2002**, *41*, 4096. [10j] T. Sheng, X. Wu, W. Zhang, Q. Wang, X. Gao, P. Lin, *Chem. Commun.* **1998**, 263. [10k] H. Adams, S. Clunas, D. E. Fenton, D. N. Towers, *J. Chem. Soc., Dalton Trans.* **2002**, 3933.

[11] [11a] P. Woodward, L. F. Dahl, E. W. Abel, B. C. Crosse, *J. Am. Chem. Soc.* **1965**, *87*, 5251. [11b] F. A. Cotton, B. H. Winquist, *Inorg. Chem.* **1969**, *8*, 1304. [11c] G. E. Lewis, C. S. Kraihanzel, *Inorg. Chem.* **1983**, *22*, 2895. [11d] A. Cornia, A. C. Fabretti, D. Gatteschi, G. Palyi, E. Rentschler, O. I. Shchegolikhina, A. A. Zhadanov, *Inorg. Chem.* **1995**, *34*, 5383. [11e] E. K. Brechin, W. Clegg, M. Murrie, S. Parsons, S. J. Teat, R. E. P. Winpenny, *J. Am. Chem. Soc.* **1998**, *120*, 7365.

[12] [12a] R. E. P. Winpenny, *Adv. Inorg. Chem.* **2001**, *52*, 1 and references cited therein. [12b] E. Diamantopoulou, C. P. Raptopoulou, A. Terzis, V. Tangoulis, S. P. Perlepes, *Polyhedron* **2002**, *21*, 2117. [12c] J. Faus, F. Lloret, M. Julve, J. M. Clemente-Juan, M. C. Munoz, X. Solans, M. Font-Bardia, *Angew. Chem. Int. Ed. Engl.* **1996**, *35*, 1485. [12d] I. G. Dance, M. L. Scudder, R. Secomb, *Inorg. Chem.* **1985**, *24*, 1201. [12e] M. Murrie, H. Stoeckli-Evans, H. U. Güdel, *Angew. Chem. Int. Ed.* **2001**, *40*, 1957.

[13] [13a] F. Birkelbach, C. Krebs, V. Staemmler, unpublished, Bochum, Germany, **1997**. [13b]D. Gatteschi, L. Pardi, *Gazz. Chim. Ital.* **1993**, *123*, 231.

[14] W. E. Hatfield, *Comments, Inorg. Chem.* **1981**, *1*, 105.

[15] A. P. Ginsberg, *Inorg. Chim. Acta Rev.* **1971**, *5*, 45.

[16] S. D. Pastor, J. D. Spivack, L. P. Steinhuebel, *J. Heterocycl. Chem.* **1984**, *21*, 1285.

[17] N. N. Timosheva, A. Chandrasekharan, R. O. Day, R. R. Holmes, *Inorg. Chem.* **1998**, *37*, 4945.

[18] T. Thompson, S. D. Pastor, G. Rihs, *Inorg. Chem.* **1999**, *38*, 4163.

[19] [19a] L. A. P. M. Hall, *Polyhedron* **1990**, *9*, 2575. [19b] V. Tangoulis, C. P. Raptopoulou, S. Paschalidou, A. E. Tsohos, E. G. Bakalbassis, A. Terzis, S. P. Perlepes, *Inorg. Chem.* **1997**, *36*, 5270.

Received March 27, 2003

